

## A periodic antiphase structure model for the intermediate plagioclases (An<sub>33</sub> to An<sub>75</sub>)

TIMOTHY L. GROVE<sup>1</sup>

Department of Geological Sciences, Harvard University  
Cambridge, Massachusetts 02138

### Abstract

Diffraction-pattern evidence and characteristics of transmission electron microscope images suggest that the intermediate plagioclase superstructure is periodic antiphase in nature. A description of the supercell utilizes the  $\bar{1}\bar{1}$ ,  $c = 14A$  subcell, and idealized models are constructed for An<sub>33</sub>, An<sub>50</sub>, An<sub>66</sub>, and An<sub>75</sub>. In the idealized models, intermediate plagioclase is a one-dimensional periodic antiphase structure that is slab-like and has a repeat unit of  $d_{\mathbf{a}}$ . Each slab consists of two halves of equal thickness that have identical ordering schemes but bear an antiphase relation to each other. The fault vector for this periodic antiphasing is  $\mathbf{R} = 1/2(\mathbf{a} + \mathbf{b})$ . Each half of the slab is composed of an albite-like layer that is Na-rich and has a low-albite tetrahedral ordering scheme, and an anorthite-like layer that is Ca-rich and has idealized  $\bar{1}\bar{1}$ ,  $c = 14A$  anorthite ordering. The antiphasing is detectable only through differences between successive anorthite-ordered regions.

The change in orientation and thickness of the slabs is revealed by the variation in location and spacing of class  $e$  satellite reflections in the intermediate-plagioclase diffraction pattern. Gay (1956) and Cole *et al.* (1951) characterized the orientation of class  $e$  reflections in An<sub>25</sub> to An<sub>75</sub> intermediate plagioclase. Reexamination of their measurements shows that the slab orientation for all compositions is nearly perpendicular to (100). Thus, the supercells are described by one translation that is nearly normal to (100) and two other translations that lie in (100) and vary in length and orientation. Models are constructed in the (100) projection which provide a simplified illustration of changes in the periodic antiphase structure as a function of composition.

### Introduction

Idealized models of intermediate plagioclase for An<sub>33</sub>, An<sub>50</sub>, An<sub>66</sub>, and An<sub>75</sub> are constructed by assuming that the superstructure is a one-dimensional periodic antiphase structure and that each periodic antiphase domain consists of an anorthite-like and an albite-like region. The existence of periodic antiphasing was suggested by Sørum (1951) and can be inferred from the diffraction pattern of intermediate plagioclase. Defect structures observed in transmission electron microscope (TEM) images (McConnell and Fleet, 1963; McConnell, 1974; Morimoto *et al.*, 1975a, b; Grove, 1976a, 1977) are also consistent with the existence of periodic antiphase domains. Structural analyses based on X-ray intensity data are consistent with the presence of Ca-rich and Na-rich do-

mains (Toman and Frueh, 1976a, b; Kitamura and Morimoto, 1975).

Reevaluation of the data of Gay (1956) and Cole *et al.* (1951) indicates that the orientations of the periodic antiphase boundaries for all intermediate plagioclases are nearly perpendicular to (100). Therefore, a supercell description is chosen that has one axis perpendicular to (100) and two axes lying in (100). This supercell is used to construct idealized structures for An<sub>33</sub>, An<sub>50</sub>, An<sub>66</sub>, and An<sub>75</sub> plagioclase.

### Diffraction geometry of intermediate plagioclase

The diffraction pattern of intermediate plagioclase contains class  $a$  reflections ( $h + k = 2n, l = 2n$ ) and a pair of  $e$  satellites that surround the position of the class  $b$  reflections ( $h + k = 2n + 1, l = 2n + 1$ ) which are absent. In plagioclase with anorthite content greater than An<sub>55</sub> a pair of  $f$  satellites surround  $a$  reflections. The  $e$  satellites are interpreted to result from a special type of superstructure that contains

<sup>1</sup> Present address: Department of Earth and Space Sciences, SUNY at Stony Brook, Stony Brook, New York 11794.

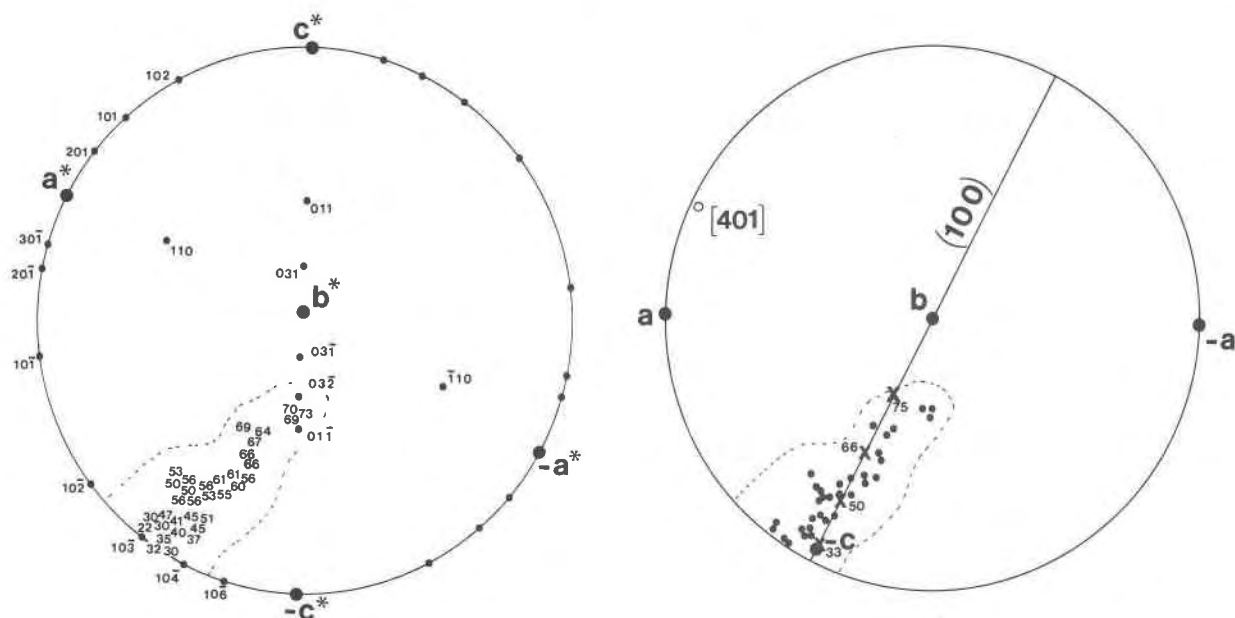


Fig. 1. (a) Orientation of  $s$  as a function of composition. Stereographic projection with  $b$  vertical. Numerals indicate the chemical composition of intermediate plagioclase. Data from Cole *et al.* (1951), Gay (1956), and Grove (1976a). (b) Deviation of  $s$  from (100). Stereographic projection using  $An_{66}$  cell dimensions.  $b$  axis is vertical. Dashed line indicates measurement uncertainty of Gay (1956).  $x$ 's are the orientations assumed in the construction of Figs. 4 and 5.

antiphase domains with  $\bar{1}\bar{1}$  symmetry. The antiphase vector is the translation  $\mathbf{R} = 1/2(\mathbf{a} + \mathbf{b})$  that is lost in the transition from  $(C\bar{1}\bar{1}, c = 7A)$  to  $(\bar{1}\bar{1}, c = 14A)$  symmetry (Müller *et al.*, 1972, 1973; McLaren and Marshall, 1974). Weak and diffuse class  $c$  ( $h + k = 2n, l = 2n + 1$ ) and  $d$  ( $h + k = 2n + 1, l = 2n$ ) reflections have also been noted in the diffraction patterns of intermediate plagioclase (Cole *et al.*, 1951). These reflections are not treated in detail in this discussion. They may represent the formation of short-range ordered An-rich domains with  $P\bar{1}$ ,  $c = 14A$  symmetry, and probably develop at low temperatures as the result of late-stage ordering processes.

The size and orientation of the intermediate-plagioclase supercell varies as a function of composition. The change in periodicity and orientation of the superstructure was characterized by Bown and Gay (1958), who described the positions of the two class  $e$  reflections about a  $b$  reciprocal lattice position by the vectors  $\mathbf{s}$  and  $-\mathbf{s}$  drawn from the  $b$  position to each  $e$  satellite:  $\mathbf{s} = \delta h\mathbf{a}^* + \delta k\mathbf{b}^* - \delta l\mathbf{c}^*$  and  $-\mathbf{s} = -\delta h\mathbf{a}^* - \delta k\mathbf{b}^* + \delta l\mathbf{c}^*$ . The class  $f$  reflections are located about class  $a$  reflections by a vector of magnitude and orientation  $2\mathbf{s}$  or  $-2\mathbf{s}$ . The change in orientation of  $\mathbf{s}$  as a function of composition is shown in stereographic projection using the data of Gay (1956), Cole *et al.* (1951) and Grove (1976b) (replotted in Fig. 1a using reciprocal lattice dimensions of  $An_{66}$  intermediate

plagioclase). Bown and Gay noted that the orientation of  $\mathbf{s}$  changed from being approximately parallel to  $[10\bar{3}]^*$  for  $An_{25}$  to approximately parallel to  $[03\bar{2}]^*$  for  $An_{75}$ . They also determined the magnitude of  $\mathbf{s}$ , the spacing between an  $e$  satellite, and the position of a  $b$  reciprocal lattice point and its reciprocal value  $1/|\mathbf{s}|$ , or  $d_b$ .

#### Characteristics of a periodic antiphase structure

A one-dimensional periodic antiphase structure consists of two slabs that are equal in thickness and bear an antiphase relation to one another. In intermediate plagioclase the slabs are oriented perpendicular to  $\mathbf{s}$ , and a complete repeat unit has a thickness  $d_b$ . In one  $d_b$  unit an antiphase boundary is encountered twice. For a periodic antiphase structure it is convenient to use the magnitude  $2\mathbf{s}$  and its reciprocal  $d_{2b}$  ( $2s$  is referred to as  $t$  and  $d_{2b}$  as  $T$  by Smith, 1974, p. 150–176, 483–496). It is only necessary to consider ordering schemes for a  $d_{2b}$  region, since the ordering scheme in the other  $d_{2b}$  region that makes up the complete  $d_b$  superstructure repeat is identical, but is in antiphase relation to the first  $d_{2b}$  region.  $d_{2b}$  also corresponds to the reciprocal of the spacing between an  $e$  satellite pair or an  $a$  reflection and an  $f$  satellite and is the periodicity observed in TEM superlattice-fringe images. The spacing  $d_{2b}$  is plotted as a function of bulk plagioclase composition in Figure 2, using the

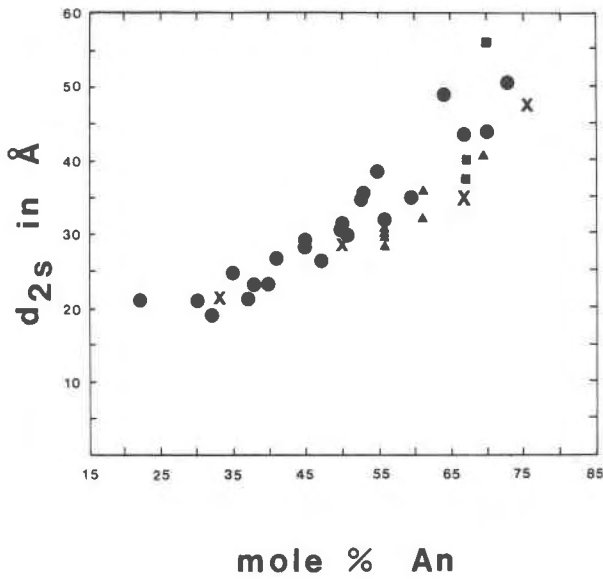


Fig. 2. Values of  $d_{2s}$  plotted as a function of chemical composition. Circles are from Gay (1956), triangles from Cole *et al.* (1951), and squares from Grove (1976a). x's are values assumed in construction of Figs. 4 and 5.

data from Gay (1956), Cole *et al.* (1951), and Grove (1976b).

One-dimensional periodic antiphase structures were first identified in copper-gold alloys by Johansson and Linde (1936) [AuCuII] and Scott (1960) [AuCu<sub>3</sub>II], and are characteristic of many binary alloy systems (Sato and Toth, 1965). The diffraction patterns of the alloys are quite similar to that of intermediate plagioclase. In addition, defect structures observed in TEM images of both intermediate plagioclase and binary alloys are very similar. The TEM images of superlattice fringes and of superstructure defects observed in the alloys CuAuII and Cu<sub>3</sub>AuII (Glossop and Pashley, 1959; Pashley and Presland, 1959; Marcinkowski and Zwell, 1963) bear a striking similarity to those observed in intermediate plagioclases (McConnell and Fleet, 1963; McConnell, 1974; Grove, 1977).

A simplified calculation can be performed to show that the diffraction pattern of intermediate plagioclase is consistent with the existence of a periodic antiphase structure. The calculation assumes: (1) the structure is a periodic antiphase structure with  $\bar{1}\bar{1}$ ,  $c = 14\text{\AA}$  subcell symmetry, and (2) the antiphase vector is  $1/2(\mathbf{a} + \mathbf{b})$ . The calculation follows that of Johansson and Linde (1936) and for simplicity the cell of plagioclase is chosen so that the  $\mathbf{c}$  translation is parallel to  $\mathbf{s}$  and the superstructure repeat  $M$  is an integral number of unit cells. Thus, the superstructure is a

slab that has a thickness of  $M$  cells. In one repeat unit of the superstructure the  $M/2$  cells along  $c$  bear an antiphase relation to the remaining  $M/2$  cells. The structure of each  $M/2$  cell layer is the same, but one layer is out-of-phase with respect to the other by the antiphase vector  $1/2(\mathbf{a} + \mathbf{b})$ . Therefore, the total scattering amplitude of the crystal can be described by:

$$E_{\text{tot}} = [\text{I.F.}][F_{\text{subcell}}] \left[ \sum_{m=1}^{M/2} \exp\left(i2\pi \frac{ml}{M}\right) + \exp(i\pi[h+k]) \sum_{m=(M/2)+1}^M \exp\left(i2\pi \frac{ml}{M}\right) \right]$$

where the expression includes the interference function (I.F.) for the superstructure and a term that sums over the  $M$  subcells (where  $m = 1, 2, 3, \dots, M$ ) of the superstructure.  $[F_{\text{subcell}}]$  is the structure factor for each  $\bar{1}\bar{1}$  subcell, and  $M/2$  of the subcells are in an antiphase relation to the first  $M/2$  subcells. Four cases must be considered for  $\bar{1}\bar{1}$  symmetry;

(1)  $h + k = 2n$  where  $l = nM$  ( $n$  an integer) with  $l$  even. Then,

$$E_{\text{tot}} = [\text{I.F.}][F_{\text{subcell}}] \left[ \sum_{m=1}^{M/2} \exp(i2\pi nM) + \sum_{m=(M/2)+1}^M \exp(i2\pi nM) \right] = [\text{I.F.}] \sum_{m=1}^M [F_{\text{subcell}}]$$

(i.e., there will be  $a$  reflections)

(2)  $h = k \neq 2n$  where  $l = nM$  ( $n$  an integer) with  $l$  odd. Then,

$$E_{\text{tot}} = [\text{I.F.}][F_{\text{subcell}}] \left[ \sum_{m=1}^{M/2} \exp(i2\pi nM) + \exp(i\pi[h+k]) \sum_{m=(M/2)+1}^M \exp(i2\pi nM) \right] = [\text{I.F.}] \left[ \sum_{m=1}^{M/2} [F_{\text{subcell}}] - \sum_{m=(M/2)+1}^M [F_{\text{subcell}}] \right] = 0$$

(i.e., there will be no intensity in the  $b$  reflection position).

For  $l \neq nM$  (the positions of satellite reflections),

$$\sum_{m=1}^{M/2} \exp\left(i2\pi \frac{lm}{M}\right) - \left[ \sum_{m=(M/2)+1}^M \exp\left(i2\pi \frac{lm}{M}\right) \right] = \frac{1 - \exp(i\pi l)}{1 - \exp\left(i2\pi \frac{l}{M}\right)}$$

The expression for the scattering amplitude becomes:

$$E_{\text{tot}} = [\text{I.F.}][F_{\text{subcell}}][1 - \exp(i\pi[h + k])] \left[ \frac{1 - \exp[i\pi l]}{1 - \exp\left[i2\pi \frac{l}{M}\right]} \right]$$

$$(3) h + k = 2n$$

$$E_{\text{TOT}} = 0$$

(i.e., no satellites about *a* reflections as a result of the antiphasing)

$$(4) h + k \neq 2n$$

for *l* even

$$E_{\text{TOT}} = 0$$

and for *l* odd

$$E_{\text{tot}} = [\text{I.F.}][F_{\text{subcell}}] \left[ \frac{4}{1 - \exp\left[i2\pi \frac{l}{M}\right]} \right]$$

(i.e., intensity in the position of the *b* reflections)

The calculation correctly predicts the observed diffraction patterns for intermediate plagioclase and shows that class *a* and *e* reflections are present and *b* reflections are absent as the result of periodic antiphasing. The calculation does not explain the presence of *f* satellites. Satellites analogous to *f*'s found in the Cu–Au alloys have been accounted for by distortions in individual antiphase domains (Glossop and Pashley, 1959). The satellites about *a* reflections have the periodicity of one periodic antiphase domain, and their presence may be related to changes in atomic positions caused by the distortions expected to occur in an individual domain near an antiphase boundary as well as by the process of ordering Ca and Na in subcells.

#### A description of the intermediate plagioclase supercell

Megaw (1960a, b, c) proposed a cell description and a structure model for intermediate plagioclase and redefined the  $C1\bar{1}$ ,  $c = 7A$  cell to a primitive cell with the translations  $1/2[311]$ ,  $1/2[110]$ , and *a*. This cell has been modified by Kitamura and Morimoto (1975), who kept the first two translations and chose a third that changed in orientation and magnitude as a function of composition.  $1/2[311]$  was chosen because Bown and Gay (1958) determined this to be the pole of the plane containing all *s* vectors. The Megaw cell adequately describes the structure, but a cell description that shows the changes in superstructure size and orientation in two dimensions would be useful. In this way it may be possible to get some insight

on superstructure ordering schemes that are consistent with the symmetry of the plagioclase subcell.

The orientation of *s* is replotted (Fig. 1b) with respect to the direct lattice translations of the 14A cell. The striking relation between the orientation of the *s* vectors and (100) is evident, and two axes of variable magnitude are chosen in this plane as required by the superstructure size for a particular composition. The lattice translation  $[401]$  is nearly perpendicular to (100) and is chosen as the third translation direction. The deviation of *s* from (100) is less than  $\pm 5^\circ$  (Fig. 3b) over the range  $An_{35}$  to  $An_{66}$ .

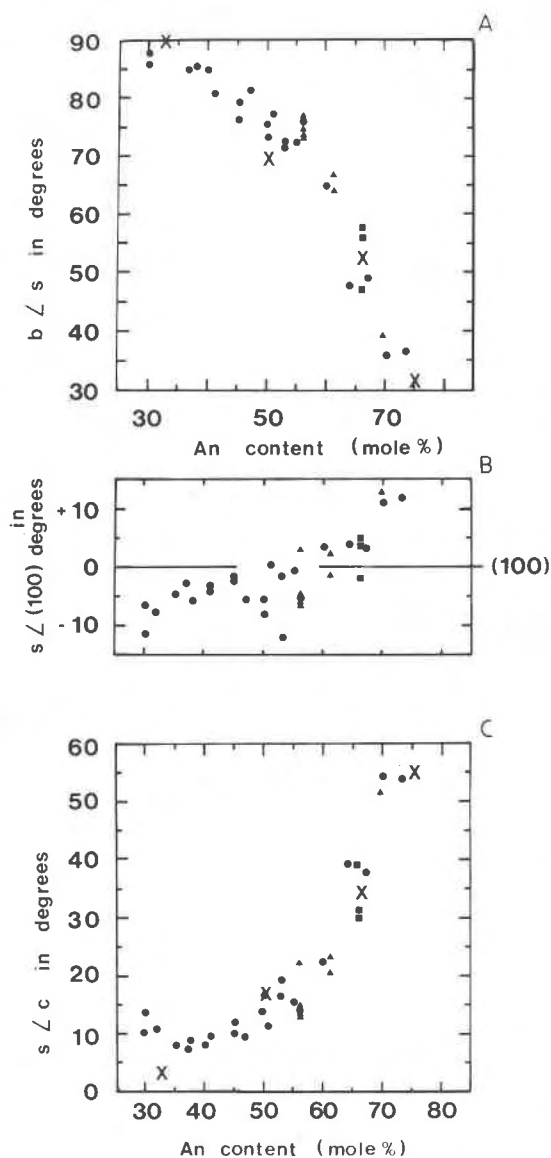


Fig. 3. (a) Angle between *s* and the *b* axis. (b) Deviation of *s* from (100) in degrees. Calculated as  $a^* \cdot s$ . (c) angle between *s* and the *c* axis. Symbols are the same as in Fig. 2.

and within  $\pm 10^\circ$  over the entire range (the uncertainties involved in the film measurement are on the order of  $\pm 10^\circ$ , Gay, 1956). A value of  $s$  determined by McLaren (1974) for  $An_{75}$  is omitted, because values for  $\delta h$ ,  $\delta k$  and  $\delta l$  are unpublished at the time of writing.

### Modeling the periodic antiphase structure

#### Previous models

The reader is referred to Smith and Ribbe (1969) and Smith (1974, p. 150–174, 483–496) for an up-to-date review of structural models for intermediate plagioclase, but some of the more significant contributions to understanding the intermediate plagioclase structure will be briefly summarized. From the time of Chao and Taylor (1940) to the present, the idea of albite-like and anorthite-like domains has been included in structural models. Some X-ray confirmation of the existence of compositional segregations comes from average structure refinements (in the  $C1^-$ ,  $c = 7A$  cell) of intermediate plagioclases. The analyses show that average cell tetrahedral-site occupancies are consistent with the presence of low albite-ordered regions in the supercell (Phillips *et al.*, 1971; Toman and Frueh, 1973a; Ribbe, 1975). On prolonged heating the  $e$  and  $f$  reflections become diffuse and weak and eventually disappear (Gay and Bown, 1956; Bown and Gay, 1969; McConnell, 1974), suggesting that the atomic arrangements involve the ordering of Al and Si atoms in tetrahedral sites. Average structure refinements have also resulted in large anisotropic temperature factors for the alkali atom sites, interpreted as positional disorder from Ca and Na ordering within the superstructure. Superstructure analyses by Toman and Frueh (1971; 1972; 1973a; b, c; 1976a, b) and Kitamura and Morimoto (1975) have succeeded in identifying the atomic coordinates of alkali atoms in individual subcells of the supercell, and show that alkali positions occupied predominantly by Ca in one portion of the structure alternate with regions occupied by Na. The structural analysis of Kitamura and Morimoto (1975) has also deduced the existence of periodic antiphasing.

#### A model based on the (100) projection

An idealized model is constructed using the inferred periodic antiphase nature of the superstructure and the (100) projection. The existence of albite-like and anorthite-like domains relies on the results of structural analyses. Supercells are chosen for the compositions  $An_{33}$ ,  $An_{50}$ ,  $An_{66}$ , and  $An_{75}$ , because

these compositions can be modeled using integral numbers of subcells in their supercell. The experimentally determined values (Fig. 3a, c) for the orientation of  $s$  are plotted on (100) along with the experimentally derived values of  $d_{2s}$  (Fig. 2), and an appropriate supercell is chosen (Fig. 4). The choice is not intended to be totally rigorous. Since there is quite a spread in reported values of  $s$ , some artistic license is exercised in the choice of cell. A continuum of supercell sizes and orientations *exists* in natural intermediate plagioclase, and the arguments made in following sections that model the superstructure in terms of ideal structural units are intended to point out the symmetry constraints on the supercell and the periodic antiphase relations. It is not the purpose of the discussion to prove that the real intermediate plagioclase superstructure corresponds to the ideal model composed of an integral number of ideally-ordered cells.

#### Alkali site ordering scheme

The (100) projection is plotted along with crystallographically-distinct Ca(00) and Ca(0z) alkali sites in the  $\bar{1}\bar{1}$  cell for  $An_{33}$ ,  $An_{50}$ ,  $An_{66}$ , and  $An_{75}$  supercells (Fig. 5). Lines plotted perpendicular to  $s$  and hence parallel to the position of the periodic antiphase boundaries are spaced every  $d_{2s}$ , the repeat unit of each periodic antiphase domain. (The periodic antiphase boundaries are vertical in this projection.) Once the orientation and spacing between periodic antiphase boundaries are determined, a structure can be guessed by filling crystallographically similar sites with either Ca or Na atoms in a manner that results in alternating anorthite-rich and albite-rich bands. Knowing the bulk composition of the phase, the correct proportions can be placed in one  $d_{2s}$  repeat unit. Note that by plotting the alkali sites it is possible to choose the number of subcells in one supercell repeat unit. The vertical cell dimension lies within the periodic antiphase boundary for all compositions. The other two translations are in the (100) plane, one chosen parallel to the periodic antiphase boundary ( $An_{33} = \mathbf{b}$ ,  $An_{50} = 3\mathbf{b} + \mathbf{c}$ ,  $An_{66} = 3\mathbf{b} + 2\mathbf{c}$ ,  $An_{75} = 3\mathbf{b} + 4\mathbf{c}$ ) and the third translation chosen parallel to  $\mathbf{c}$  ( $An_{33} = 3\mathbf{c}$ ,  $An_{50} = 4\mathbf{c}$ ,  $An_{66} = 6\mathbf{c}$ ,  $An_{75} = 12\mathbf{c}$ ). The complete cells are shown in Figure 4, and ordering schemes for one-half of the cell are shown in the alkali site projection (Fig. 5).

It is only necessary to show a  $d_{2s}$  unit of the complete cell ( $d_s$ ), since the ordering scheme proposed for the first portion is in antiphase relation to the second portion by  $\mathbf{R} = \frac{1}{2}(\mathbf{a} + \mathbf{b})$ . For the alkali sites this

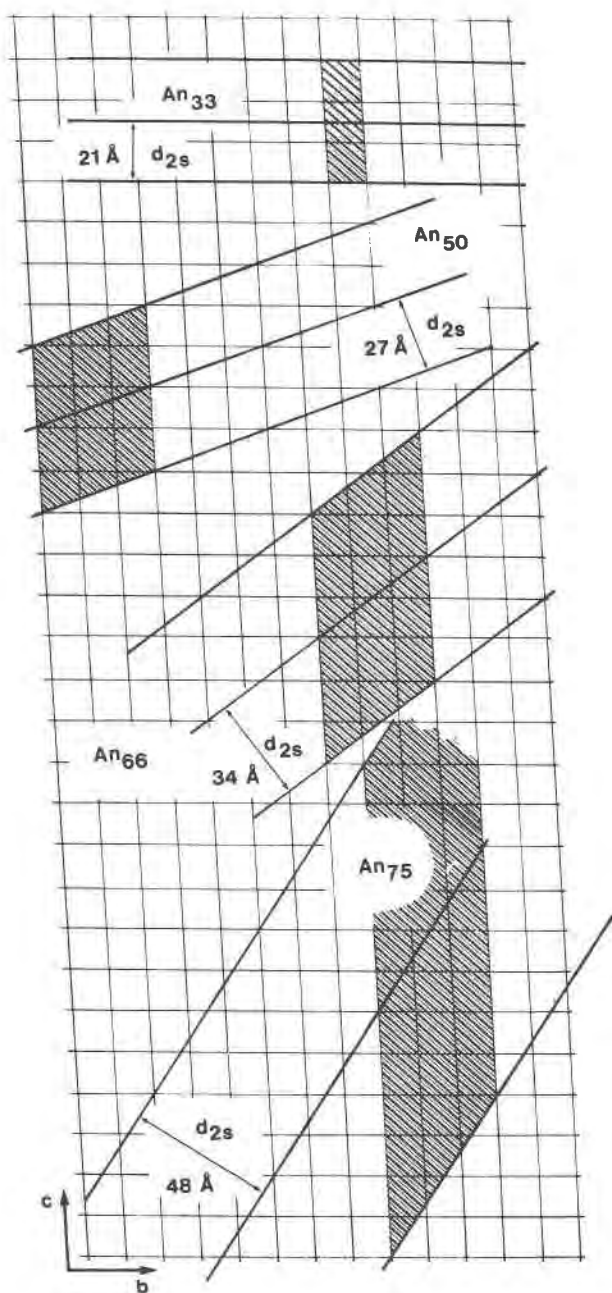


Fig. 4. Cells chosen to describe the intermediate-plagioclase superstructure. A complete  $d_s$  unit is shown in the (100) projection.

means that the atomic positions of the Na atoms in the first  $d_{2s}$  portion and the second faulted  $d_{2s}$  portion are indistinguishable. The atomic positions of Ca in the second faulted  $d_{2s}$  portion will be displaced with respect to the atoms in the first  $d_{2s}$  region by the deviation of crystallographically distinct  $Ca_{(00)}$  sites and  $Ca_{(0z)}$  sites in an  $I\bar{1}$  cell from their  $C\bar{1}$  average position. Thus, the two  $d_{2s}$  portions have the same

ordering scheme, but in terms of atomic site coordinates the positions of the Ca atoms in the first  $d_{2s}$  portion of the cell will not superimpose with the second portion. If the Na-rich portion of the superstructure has the albite structure, there will be no difference between the first  $d_{2s}$  albite-like region and the second  $d_{2s}$  albite-like region.

#### Consequences of periodic antiphasing

The consequence of periodic antiphasing in terms of the alkali atom positions is to slightly shift the Ca atoms. The small differences in alkali site positions between a  $d_{2s}$  unit and its faulted equivalent are not known in detail, but the  $I\bar{1}$  aspects of the tetrahedral equipoints show the antiphasing very well. There are four crystallographically-distinct tetrahedral sites in ideal low-albite, of which  $T_{10}$  contains all the Al atoms and  $T_{1m}$ ,  $T_{20}$  and  $T_{2m}$  contain only Si. The loss of symmetry that results in ordering anorthite on the  $I\bar{1}$ ,  $c = 14A$  scheme generates two crystallographically distinct sites,  $T_{100}$  and  $T_{10z}$ , etc. for a total of eight crystallographically distinct tetrahedral

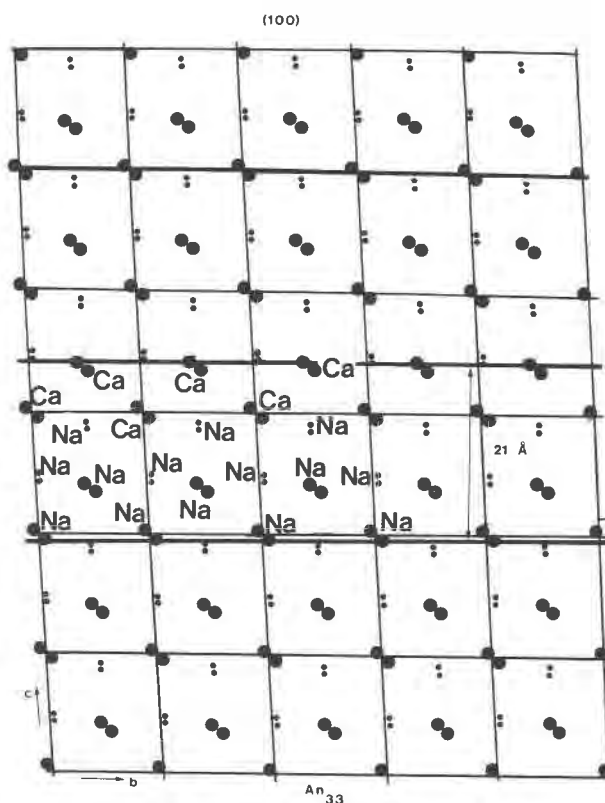
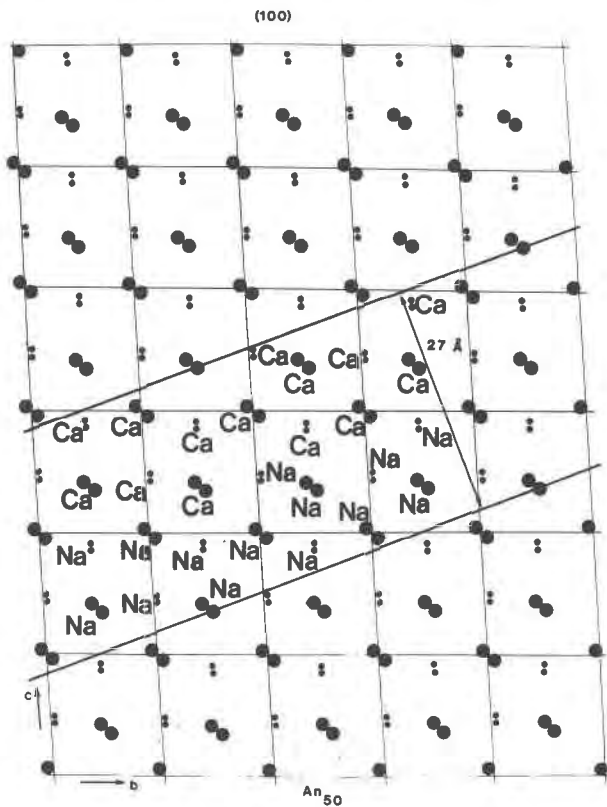
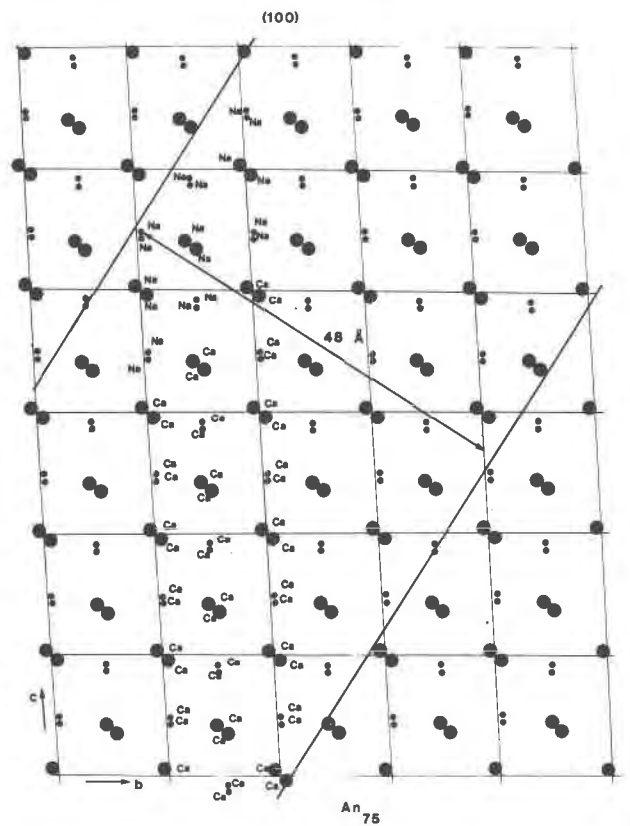
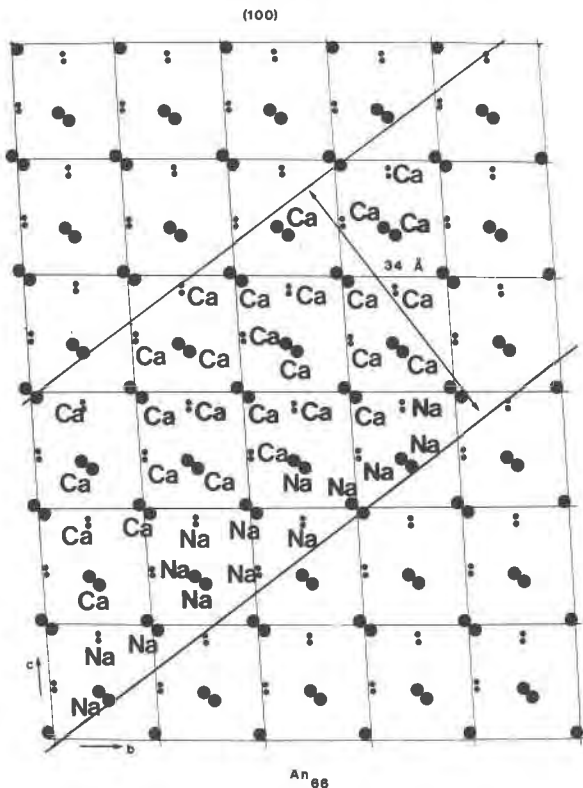


Fig. 5a. (100) projection of the alkali sites using the  $I\bar{1}$  cell. Small circles are  $Ca_{000}$ , large circles are  $Ca_{020}$ . Superstructure periodicity and orientation are taken from Figs. 2 and 3;  $b$  and  $c$  axes lie in plane of paper,  $[401]$  is vertical. An<sub>33</sub>. (b) An<sub>50</sub> (c) An<sub>66</sub> (d) An<sub>76</sub>.

Fig. 5b. (100) projection,  $An_{50}$ .Fig. 5d. (100) projection,  $An_{75}$ .Fig. 5c. (100) projection,  $An_{66}$ .

sites. In an ideally ordered  $\bar{1}\bar{1}$ ,  $c = 14A$  anorthite structure, half the sites contain Al, half contain Si, and all  $T-O-T'$  bonds are the type Al-O-Si. No change results when the antiphase vector [ $R = \frac{1}{2}(a + b)$ ] operates on the albite-ordered region, because  $\frac{1}{2}(a + b)$  is a symmetry element of the  $C\bar{1}$ ,  $c = 7A$  albite ordering scheme. However, the effect of carrying out the antiphase operation on the  $\bar{1}\bar{1}$  anorthite-ordered framework is to reverse the Al/Si occupancies of the tetrahedral sites and change the positions of the oxygen atoms.

An example of the tetrahedral-site distribution for an idealized  $An_{50}$  superstructure is shown in Figure 6. Tetrahedral sites that contain Al are shown in gray, and those containing Si are white. Choose a tetrahedral site in the anorthite-ordered region (e.g.,  $a$  in Fig. 6) that contains Si, now translate to the anorthite region in the next periodic antiphase domain. The tetrahedral site occupancy is reversed ( $a'$  now contains Al), and Si-bearing tetrahedra in the first anorthite region are occupied by Al in the antiphase-related region. Carrying out a similar operation in an albite ordered region ( $b$ ) and the next fault-related albite region ( $b'$ ) shows that antiphasing does not

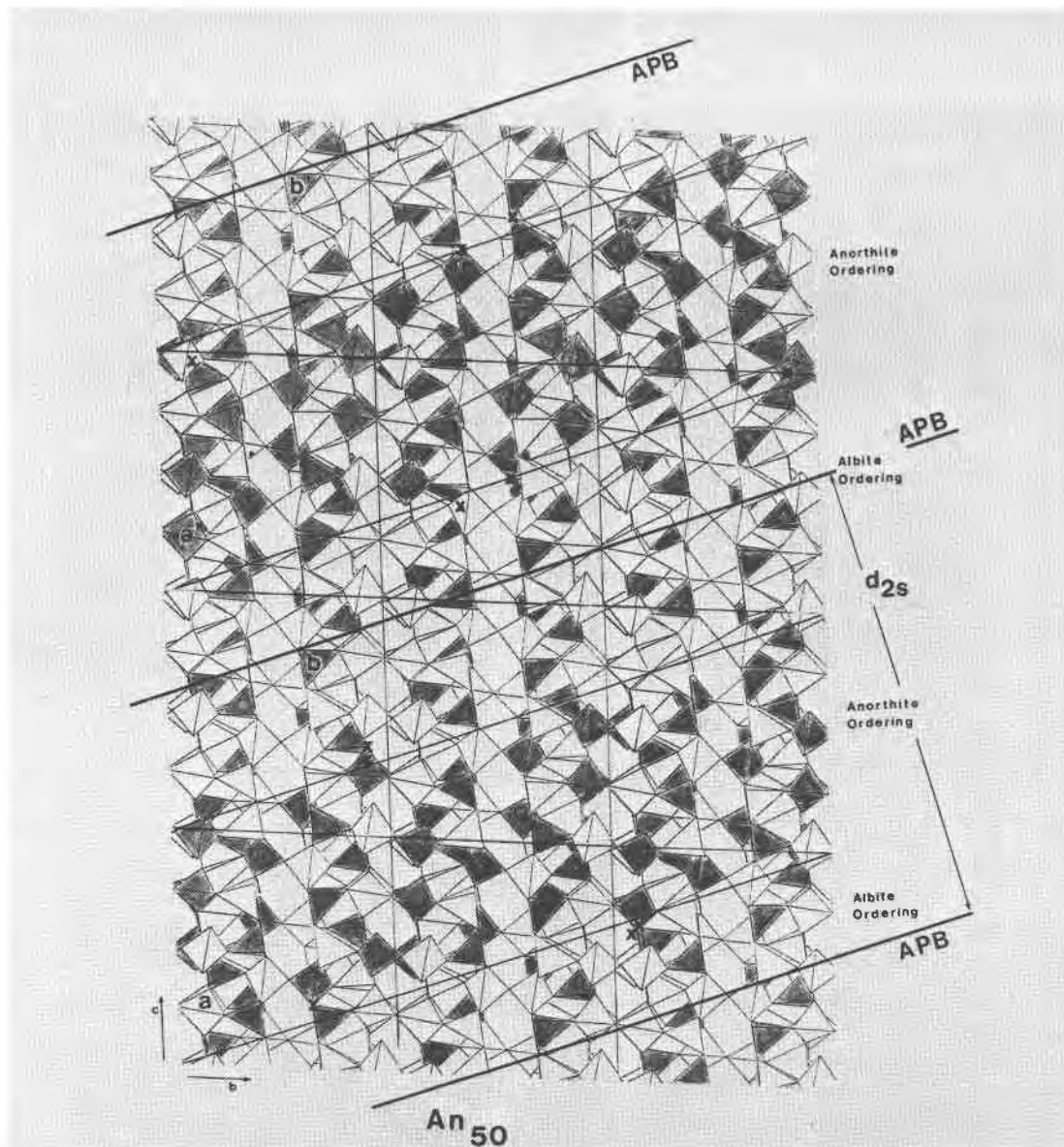


Fig. 6. (100) projection showing the tetrahedra in the  $An_{50}$  superstructure model. Dark tetrahedra contain Al. Light tetrahedra contain Si. The positioning of the APB is arbitrary and only needs to be chosen within the albite region.

affect this  $C\bar{1}$ -ordered portion of the supercell unit. It does not seem necessary to designate any particular plane within the superstructure as an antiphase boundary (APB), and it seems adequate to choose it somewhere inside the albite region and then at the same position in each successive  $d_{2s}$  unit. The many beam direct-lattice images of Morimoto *et al.* (1975a) splendidly show this aspect of the intermediate plagioclase structure. Their Figures 2 and 3 show regions in which antiphasing is not detectable (albite-like) and regions in which it is present (anorthite-like). A result of connecting the low albite-ordered and  $I\bar{1}$  anorthite-ordered frameworks is to generate

Al–O–Al bonds (marked by  $x$ 's in Fig. 6). This is an unavoidable consequence, because the aluminum-bearing  $T_0$  sites in albite will connect to tetrahedra in the anorthite portion that contain both Al and Si atoms, and the ideal model results in Al–O–Al bonds. Al–O–Al bonds are avoided when possible, as shown by the existence of only Al–O–Si bonds in  $I\bar{1}$  and  $P\bar{1}$ -ordered anorthite (Megaw *et al.*, 1962) and margarite (Bailey, 1975). The evidence from Kitamura and Morimoto's structure solution suggests that the composition of the Ca-rich and Na-rich regions of the structure are  $An_{80}$  and  $An_5$ , respectively. This may give rise to an averaging in the real structure of



intermediate plagioclase and allow Al–O–Al bonds to be successfully avoided. Thus, the problem of generating Al–O–Al bonds at every albite–anorthite interface encountered by this ideal model suggests that the real intermediate plagioclase structure does not approach the idealized configuration of pure Ca and Na regions.

The superstructure models allow some speculation on the compositional range over which intermediate plagioclase is present. The idealized model for  $An_{33}$  represents a lower limit for a scheme consistent with anorthite–albite regions ordered on  $\bar{1}\bar{1}$  subcell symmetry. The next most likely ordering scheme is pure  $C\bar{1}$ ,  $c = 7A$  albite. Since the assumption of pure albite and pure anorthite domains is probably incorrect, intermediate-plagioclase structures may exist for compositions less calcic than  $An_{33}$ , but a careful characterization of the peristerite two-plagioclase intergrowths must be made before absolute limits can be set. It appears that one could construct larger and larger ordered periodic antiphase structures for the calcic intermediate plagioclase, and evidence for long-period superstructures is suggested by the large  $d_{28}$  measured in an  $An_{75}$  specimen by McLaren (1974). Transmission electron microscope studies (Grove, 1977) confirm that the same limit set by Cole *et al.* (1951) of  $An_{75}$  is a likely upper limit for intermediate plagioclase. In addition, the TEM observations reveal that plagioclase with bulk composition in the range  $An_{66}$  to  $An_{90}$  consists of complex two-phase intergrowths of  $\bar{1}\bar{1}$  bytownite and intermediate plagioclase of variable  $s$ .  $An_{66}$  intermediate plagioclase and  $An_{87}$  bytownite ( $P\bar{1}$ ,  $c = 14A$ ) intergrowths are found in plagioclase samples that cooled under metamorphic conditions, and this coexisting pair may represent the closest approach to equilibrium. [The results of Voll may indicate that even greater degrees of equilibration exist (Smith, 1972).] Thus, any plagioclase in the  $An_{66}$  to  $An_{75}$  range must be characterized carefully, since it may be a two-phase intergrowth consisting of intermediate plagioclase and a calcic bytownite.

#### Acknowledgments

Financial support for this study was provided by National Science Foundation Grants GA12852 and GA41415 to C. W. Burnham. The author thanks C. W. Burnham, J. B. Thompson, Jr., David Kohlstedt, John Ferry, and Robert Hazen for many stimulating discussions on plagioclase. Reviews by Paul Ribbe and Wayne Dollase considerably improved the manuscript. The author also thanks Masao Kitamura for discussion about his intermediate-plagioclase structural studies.

#### References

- Bailey, S. W. (1975) Cation ordering and pseudosymmetry in layer silicates. *Am. Mineral.*, *60*, 175–187.
- Bown, M. G. and P. Gay (1958) The reciprocal lattice geometry of the plagioclase feldspar structures. *Z. Kristallogr.*, *111*, 1–14.
- and P. Gay (1969) The effect of heat treatment on the diffraction patterns of intermediate plagioclases. *Z. Kristallogr.*, *129*, 451–457.
- Chao, S. H. and W. H. Taylor (1940) Isomorphous replacement and superlattice structures in the plagioclase feldspars. *Proc. R. Soc. (London)*, *A176*, 76–87.
- Cole, W. F., H. Sörum and W. H. Taylor (1951) The structures of the plagioclase feldspars. I. *Acta Crystallogr.*, *4*, 20–29.
- Gay, P. (1956) The structures of the plagioclase feldspars: VI. Natural intermediate feldspars. *Mineral. Mag.*, *31*, 21–40.
- and M. G. Bown (1956) The structures of the plagioclase feldspars: VII. The heat treatment of intermediate plagioclases. *Mineral. Mag.*, *31*, 306–313.
- Glossop, A. B. and D. W. Pashley (1959) The direct observation of antiphase domain boundaries in ordered copper gold (CuAu) alloy. *Proc. R. Soc. (London)*, *A250*, 132–146.
- Grove, T. L. (1976a) Exsolution in metamorphic bytownite. In H.-R. Wenk *et al.*, Eds., *Electron Microscopy in Mineralogy*, p. 266–270. Springer-Verlag, Berlin.
- (1976b) *Structural Characterization of Natural Calcic Plagioclases*. Ph.D. thesis, Harvard University.
- (1977) Structural characterization of labradorite–bytownite plagioclase from volcanic, plutonic and metamorphic environments. *Contrib. Mineral. Petrol.*, in press
- Johansson, C. H. and J. O. Linde (1936) Röntgenographische und elektrische Untersuchungen des CuAu systems. *Ann. Physik*, *25*, 1–48.
- Kitamura, M. and N. Morimoto (1975) The superstructure of intermediate plagioclase. *Proc. Japan Acad.*, *51*, 419–424.
- Marcinkowski, J. F. and L. Zwell (1963) Transmission electron microscopy study of the off-stoichiometric  $Cu_3Au$  superlattices. *Acta Metall.*, *11*, 373–390.
- McConnell, J. D. C. (1974) Analysis of the time-temperature transformation behavior of the plagioclase feldspars. In W. S. MacKenzie and J. Zussman, Eds., *The Feldspars*, p. 460–477. Manchester University Press, Manchester.
- and S. G. Fleet (1963) Direct electron optical resolution of antiphase domains in a silicate. *Nature*, *199*, 586.
- McLaren, A. C. (1974) Transmission electron microscopy of the feldspars. In W. S. MacKenzie and J. Zussman, Eds., *The Feldspars*, p. 378–423. Manchester University Press, Manchester.
- and D. B. Marshall (1974) Transmission electron microscope study of the domain structures associated with the  $b$ -,  $c$ -,  $d$ -,  $e$ - and  $f$ -reflections in plagioclase feldspars. *Contrib. Mineral. Petrol.*, *44*, 237–250.
- Megaw, H. D. (1960a) Order and disorder. I. Theory of stacking faults and diffraction maxima. *Proc. R. Soc. (London)*, *A259*, 59–78.
- (1960b) Order and disorder. II. Theory of diffraction effects in the intermediate plagioclase feldspars. *Proc. R. Soc. (London)*, *A259*, 159–183.
- (1960c) Order and disorder. III. The structure of the intermediate plagioclase feldspars. *Proc. R. Soc. (London)*, *A259*, 184–202.
- , C. J. E. Kempster and E. W. Radoslovich (1962) The

- structure of anorthite,  $\text{CaAl}_2\text{Si}_2\text{O}_8$ . II. Description and discussion. *Acta Crystallogr.*, *15*, 1017-1035.
- Morimoto, N., Y. Nakajima and M. Kitamura (1975a) Direct observation of the superstructure of labradorite by electron microscopy. *Proc. Japan Acad.*, *51*, 725-728.
- , Y. Nakajima and M. Kitamura (1975b) Antiphase relations in superstructures of the *e* plagioclase. *Proc. Japan Acad.*, *51*, 729-732.
- Müller, W. F., H.-R. Wenk and G. Thomas (1972) Structural variations in anorthites. *Contrib. Mineral. Petrol.*, *34*, 304-314.
- , H.-R. Wenk, W. L. Bell and G. Thomas (1973) Analysis of the displacement vectors of antiphase domain boundaries in anorthites ( $\text{CaAl}_2\text{Si}_2\text{O}_8$ ). *Contrib. Mineral. Petrol.*, *40*, 63-74.
- Pashley, D. W., and A. E. B. Presland (1959) The observation of antiphase boundaries during the transition from CuAuI to CuAuII. *J. Inst. Metals*, *87*, 419-428.
- Phillips, M. W., A. A. Colville and P. H. Ribbe (1971) The crystal structures of two oligoclases: a comparison with low and high albite. *Z. Kristallogr.*, *133*, 43-65.
- Ribbe, P. H. (1975) The chemistry, structure and nomenclature of feldspars. In P. H. Ribbe, Ed., *Feldspar Mineralogy*, R1-R72. *Mineral. Soc. Am. Short Course Notes*, *2*.
- Sato, H. and R. S. Toth (1965) Long period superlattices in alloys. In T. B. Massalski, Ed., *Alloying Behavior and Effects in Concentrated Solid Solutions*, p. 295-419. Gordon and Breach, New York.
- Scott, R. E. (1960) New complex phase in the copper-gold system. *J. Appl. Phys.*, *31*, 2112-2117.
- Smith, J. V. (1972) Critical review of synthesis and occurrence of plagioclase feldspars and a possible phase diagram. *J. Geol.*, *80*, 505-525.
- (1974) *Feldspar Minerals. I. Crystal Structure and Physical Properties*. Springer-Verlag, New York.
- and P. H. Ribbe (1969) Atomic movements in plagioclase feldspars: kinetic interpretation. *Contrib. Mineral. Petrol.*, *21*, 157-202.
- Sørum, H. (1951) Studies on the structures of plagioclase feldspars. *Norske Videnskap Selskabs Skrifter* 1951, *3*, 1-160.
- Toman, K. and A. J. Frueh (1971) On the origin of plagioclase satellite reflections. *Acta Crystallogr.*, *B27*, 2182-2186.
- (1972) Intensity averages of plagioclase satellites: distribution in reciprocal space. *Acta Crystallogr.*, *B28*, 1657-1662.
- (1973a) On the centrosymmetry of intermediate plagioclases. *Z. Kristallogr.*, *138*, 337-342.
- (1973b) The intensities and Fourier transforms of difference reflections. *Acta Crystallogr.*, *A29*, 121-127.
- (1973c) Patterson function of plagioclase satellites. *Acta Crystallogr.*, *A29*, 127-133.
- (1976a) Modulated structure of an intermediate plagioclase: I. Model and computation. *Acta Crystallogr.*, *B32*, 521-525.
- (1976b) Modulated structure of an intermediate plagioclase. II. Numerical results and discussion. *Acta Crystallogr.*, *B32*, 526-538.

*Manuscript received, March 10, 1976, accepted  
for publication, June 1, 1977.*